Journal of Building Engineering 62 (2022) 105356

Contents lists available at ScienceDirect

Journal of Building Engineering

journal homepage: www.elsevier.com/locate/jobe

Carbon sequestration in graphene oxide modified cementitious system

Geetika Mishra [*], Ashraf Warda, Surendra P. Shah

Center for Advanced Construction Materials, Department of Civil Engineering, The University of Texas at Arlington, USA

ARTICLE INFO

Keywords:
Graphene oxide
CO_2 sequestration
Hydration
Calcium carbonate
Accelerated carbon curing

ABSTRACT

Graphene oxide is emerging as a promising nanomaterial owing to its unique property of being a strong and flexible material. This work examines the potential use of graphene oxide (GO) for CO_2 sequestration in cementitious-based materials in addition to mechanical properties. The effect of oxidized graphene surface on the hydration mechanism of cement paste and carbonate mineralization was investigated. Experimental results show that the application of GO at optimum amount offers 40% improvement in compressive strength at an early age. Accelerated carbon curing of GO-cement matrix was performed to evaluate CO_2 sequestration through thermogravimetric analysis and results revealed that adding a low concentration of GO (i.e. 0.05%) improved CO_2 uptake by 30% in the cementitious system. Further, physical adsorption of CO_2 molecules and alteration in C–S–H was confirmed by the FTIR study. This finding suggests that the application of GO, not only improved the mechanical properties but it significantly enhanced the CO_2 sequestration in cementitious systems.

1. Introduction

Carbon-based materials have been widely used to improve various aspects of cement-based materials in recent years [1–3]. Graphene oxide (GO) is a two-dimensional carbon-based material that has attracted worldwide attention due to its potential characteristics such as high reactivity and stability, high specific surface area, and outstanding mechanical properties [4]. This material comes from exfoliation of the graphite by chemical route, where the resulting material is functionalized sheets with oxygenated groups localized to a greater extent on sheet edges and the basal plane. The existing research on the performance of cement-based materials considered the addition of GO up to 0.1% by weight of cement and found that it has a huge potential to improve the mechanical and durability properties of cementitious systems [5,6].

Recent years witnessed that the construction industry is one of the sectors where carbon dioxide (CO_2) emission is a serious concern. According to an estimate, about one ton of CO_2 is released into the atmosphere during the production of one ton of Portland cement [7]. Carbon sequestration in cementitious materials is one of the potential solutions to the problem of growing emissions. The normal carbonation process is controlled by the diffusivity of CO_2 and its reactivity with a cementitious matrix [8]. Several researchers have explored the use of supplementary materials such as fly ash, slag, metakaolin, silica fume, and a range of nanomaterials to resist carbonation in hydrated cement matrixes and it is attributed to the refinement of pore structure and reduction of calcium hydroxide (CH) due to pozzolanic reaction and transforming to C–S–H [9–11]. The carbonation of cementitious materials can be classified into two different types (natural or accelerated) depending on material type, CO_2 concentration, and exposure time [12]. Natural

---

[*] Corresponding author.
E-mail addresses: geetika.mishra@uta.edu (G. Mishra), warda.ashraf@uta.eduand (A. Warda), surendra.shah@uta.edu (S.P. Shah).

https://doi.org/10.1016/j.jobe.2022.105356
Received 23 July 2022; Received in revised form 16 September 2022; Accepted 29 September 2022

carbonation is a slow and long-term process (low CO_2 concentration, 0.0415% or 415 ppm), which is not viable to access the potential of materials for carbon capture in the scenario of increasing cement demand [13]. Hence, the accelerated carbonation may make it easier to monitor CO_2 uptake in short term. Accelerated carbonation is a fast process that uses a high CO_2 concentration (>3%) to accelerate the hydration process and produce carbonates [14,15]. In this way, it also promotes CO_2 sequestration in cementitious materials. In addition to addressing the environmental and economic benefits of capturing CO_2, accelerated carbon curing of cementitious materials improved mechanical, microstructural, and durability properties [16–18].

In general, when cementitious material is exposed to atmospheric CO_2, It diffuses and hydrolyzes to bicarbonate (HCO_3^-) and carbonate ions (CO_3^{2-}) in the alkaline porous solution of cement matrix as follows:

$$CO_2^- + OH\text{–}\ HCO_3^-$$

$$HCO_3^{2-}\ CO_3^{2-} + H^+$$

$$Ca^{2+}\ \text{(in pore solution)} + CO_3^{2-}\ CaCO_3$$

Additionally, these carbonate ions precipitate as calcium carbonate after consuming the calcium ions from hydration products in the cement matrix [19,20]. The carbonation process strongly depends on the transport medium and in a cement matrix amount of water is a crucial factor. The excess amount of water present in the voids may cause a reduction in the ingress of CO_2, while at the same time, sufficient water is essential for calcium and carbon dioxide to dissolve and react.

The improvement in degree of hydration from 56.9% to 65.4% after 28 days with the addition of 0.2 wt% of GO revealed that GO can increase cement hydration but marginally improves the degree of C–S–H gel polymerization [21]. According to research on the pore structure of GO-cement paste [22], GO had a significant impact on the gel pores in the early stages of hydration, and the total pore volume of the gel pores was reduced as GO concentration increased. Several studies have reported the effect of GO on hydration, mechanical, and durability properties, while to the best of the authors' knowledge, this is the first comprehensive evaluation of the carbon sequestration ability of graphene oxide and its effect on the developing mechanical properties of GO-cement matrix. Based on that, the main objective of this paper is to elucidate the mechanism of the interaction of GO with calcium-bearing phases in cementitious systems under accelerated carbonation conditions. Furthermore, effects on strength, CO_2 uptake, carbonate mineralization, and FTIR analysis of graphene oxide added sample was also assessed to understand the potential of GO for carbon capture and maintaining its structural integrity compared to plain cement-based materials.

2. Materials and methods

2.1. Materials

In this study, specimens were prepared using Type I ordinary Portland cement (OPC) 42.5 R. Chemical composition of cement is illustrated in Table 1. Graphene oxide was procured from Sigma Aldrich and had a bulk density of ~1.8 g/cm^3. According to the provider, graphene oxide consists of 15–20 exfoliated graphene nanoplatelets containing mostly hydroxyl (-OH) functional groups, which allows it to disperse in water for further chemical modifications. The functionalization groups are attached to the border of the layers, aiming to preserve the intrinsic properties of graphene (e.g. electric conductivity). XRD analysis shows an intense peak at 26.2 (2 theta), probably due to the partial oxidation of natural graphite flakes to graphene, in Fig. 1.

2.2. Sample preparation

In the present work, cement paste specimens with the addition of graphene oxide (0%, 0.05%, and 0.1%) were prepared for two curing conditions such as carbon curing and water curing. All the samples were prepared at w/c ratio of 0.5. The higher w/c ratio was considered to produce a workable mix. A standard Hobert mixer capable of operating from 140 to 285 rpm was employed. In the process of preparing the GO suspension, GO was first mixed with de-ionized water in a beaker at 1000 rpm for 60 min under a shear mixer and afterward, cement was combined with the GO suspension to mix for an additional 3–4 min at 285 rpm. After the completion of the procedure, the mixture was cast in 25 mm cube molds for mechanical and microstructural testing. Following demolding after 24 h, a few samples were cured in water at 23 °C temperature till the time of testing, while the same number of samples were transferred to the carbonation chamber, controlled at 20% CO_2 (100% purity) supplied at 15 Psi, 25 ± 2 °C temperature and 75 ± 5% relative humidity to evaluate carbon capture capacity. High relative humidity supplies enough moisture for the carbonation process [23–25].

Table 1
Chemical Composition of cement used in the study.

Components	Quantity (%)
CaO	66.9
SiO_2	19.5
Al_2O_3	3.52
Fe_2O_3	3.37
SO_3	3.97
$Na_2O + K_2O$	1.53
MgO	0.68
TiO_2	0.21
P_2O_5	0.1

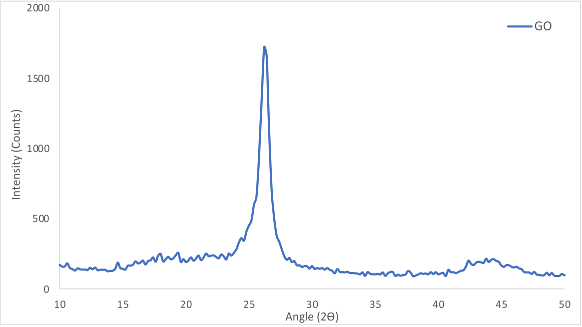

Fig. 1. XRD profile of graphene oxide.

The samples were tested from both the curing system after 7 and 28 days. For further instrumental investigation, samples were extracted after compression testing of each sample and soaked in isopropanol for 5 days to stop hydration, followed by storing in a vacuum desiccator to avoid any further hydration/carbonation reactions. Table 2 includes details on the samples studied.

2.3. Experimental methods

Heat of hydration was measured on fresh paste samples, using an isothermal conduction calorimeter (I-Cal Flex, Calmetrix, USA). Cement and graphene oxide suspension were preconditioned for 24 h at 23 °C, prior to the experiment. Then the preconditioned materials were mixed in a plastic ampoule (about 26 g of mixed paste) outside the calorimeter for 3 min using a high-speed paste mixer, as per ASTM C1679. Heat of hydration and cumulative heat evolutions are plotted for the initial 30 h after normalizing with respect to the cement mass.

TGA was performed to determine chemically bound water (BW) and degree of hydration (DOH) on uncarbonated (water cured) and carbonated (CO_2 cured) samples (at 7 and 28 days). For carbonated samples, calcium carbonate and calcium hydroxide were also determined at 7 and 28 days. Before the TGA test, approximately 40 mg of the paste was cored and then wet ground with isopropanol to stop the hydration [26]. Measurements were carried out in the temperature range from 20 °C to 900 °C at the rate of 15 °C/min purging N_2 gas during the heating process. TGA was done on two samples in each mix to check for variance in the carbonation process, and because of less than 1% variation, further tests were performed with one sample only. BW and DOH were calculated according to the Bhatty's method [27] based on the weight change between 105 °C and 900 °C using Eqs. (1) and (2)

$$BW = W_{dh} + W_{dx} + 0.41(W_{dc}) \tag{1}$$

$$DOH = \frac{W_{dh}}{0.23} \times 100 \tag{2}$$

Where, Wdh, Wdx, and Wdc are mass losses due to dehydration (75–400 °C), de-hydroxylation (400–500 °C) and decarbonization (550–900 °C) respectively. The factor 0.41 is used to convert the mass loss due to decarbonization to equivalent molecular weight of water in portlandite. In Eq. (2), According to the Bogue's formulae [28], 0.23 is the amount of chemically bound water at complete hydration calculated from the theoretical stoichiometry of cement. The content of calcium hydroxide (CH), calcium carbonate ($CaCO_3$), and CO_2 uptake were calculated using equations (3)–(5) [29].

$$CH(g/100g) = \frac{M_{400} - M_{500}}{M_{105}} \times 4.1 \times 100 \tag{3}$$

$$CaCO_3(g/100g) = \frac{M_{525} - M_{900}}{M_{105}} \times 2.27 \times 100 \tag{4}$$

$$CO_2\ uptake\ (\%) = \frac{M_{CO_2-carbonated}\ (wt\%)}{100 - M_{CO_2-carbonated}\ (wt\%)} \times 100 \tag{5}$$

Where M_{400}, M_{500}, M_{525} and M_{900} are the masses (g) of the samples at the given temperatures and $M_{CO2\text{-}carbonated}$ refers to the ratio of mass loss of carbonated sample due to $CaCO_3$ decomposition to dry mass of the sample at 105 °C. Also, 4.1 is the molar weight ratio of

Table 2
Mix details of the samples.

S.No.	Mixes	Cement	GO	w/c
1	Cement paste	100%	0	0.5
2	C + G05	99.95%	0.05%	0.5
3	C + G1	99.90%	0.1%	0.5

$Ca(OH)_2$ to H_2O, and 2.27 is the molar weight ratio of $CaCO_3$ to CO_2.

The compressive strength of water and CO_2 cured specimens was measured after 7 and 28 days using a displacement rate of 0.02 mm/s. An average of five specimens was taken as a result. In addition, surface charge (zeta potential) of GO suspension, saturated $Ca(OH)_2$, and combined GO + CH solutions were determined using the Zetasizer Ultra instrument based on Dynamic Light Scattering (DLS) and Electrophoretic Light Scattering (ELS) system. Furthermore, to observe the interaction of $Ca(OH)_2$ and GO under CO_2 environment, the solutions of GO (similar to the amount added in cementitious specimens) and saturated $Ca(OH)_2$, about 15 ml were mixed and transferred to a controlled carbonation chamber at a CO_2 concentration of 20% for 24 h. To verify the effect of carbonation on individual solutions, GO and saturated $Ca(OH)_2$ (10 ml) were also placed independently in the carbonation chamber.

For FTIR measurement, the IR spectra were carried out on attenuated total reflection mode at the resolution of 4 cm^{-1} with 32 scans per sample.

3. Results and discussions

3.1. Heat of hydration of GO-modified cement

The impact of GO on the hydration of cement was shown in Fig. 2. The graph shows that the addition of GO increased the heat of hydration of cement. This is explained by the fact that, as water starts the hydration process of cement, GO acts as a catalyst for hydration by attracting water molecules and creating nucleating sites for the hydration process to begin on its surface. The exothermic peak and the rate of heat released were observed higher in GO-added cement paste. The shoulder peak near 8 h and 12 h was more pronounced, which indicates the accelerating effect of the GO to promote cement hydration, similar results were confirmed by Li et al. [30]. Also, in Fig. 2 (b), with the progress of the hydration time heat released was observed higher on adding both doses of GO (0.05% and 0.1%) compared to plain cement. This may be caused probably due to the contribution of oxygen-containing functional groups on GO surface, which helped in homogenous dispersion of GO and promoted precipitation of hydration products. Similar hydration behavior is shown with the addition of 0.05% and 0.1% of graphene oxide with time.

3.2. Degree of hydration

Chemically Bound water (BW) was calculated from TGA at 7 and 28 days of hydration in uncarbonated (water cured) and carbonated (CO_2 cured) cement paste, illustrated in Table 3. In general, the amount of BW increases with the time of hydration. However, in this study, it was observed that the BW decreased in G1 blended cement only at later ages.

At the age of 7 days, the increase in BW is 3–4% in GO-added samples on exposure to CO_2, compared to plain cement paste. This is

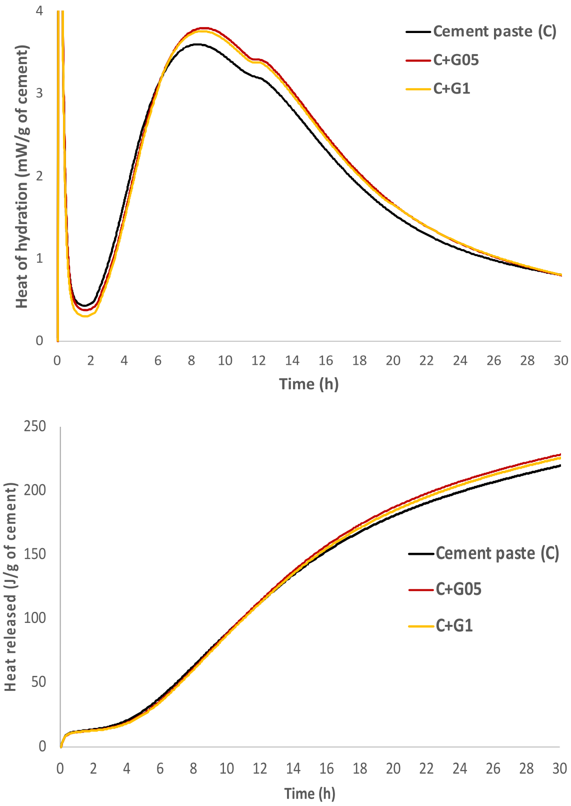

Fig. 2. Heat of hydration curves.

Table 3
Bound water in uncarbonated and carbonated cement paste.

	Bound water (%)			
Mix	**7d-Uncarbonated**	**7d-Carbonated**	**28d-Uncarbonated**	**28d-Carbonated**
Cement paste (CP)	15	15.66	15.56	15.91
CP + G05	14.31	16.18	16.40	16.86
CP + G1	14.37	16.21	16.62	16.18

ascribed to accelerated carbon curing. Early carbonation leads to accelerated hydration kinetics, which resulted in more hydration products. However, at 28 days, in uncarbonated G05 and G1, BW increased by 5.39% and 6.81%, respectively compared to plain cement while in carbonated conditions, G05 showed an increase of 5.97% and G1 showed a marginal increase of 1.69% chemically bound water compared to plain cement. It is accounted for a coating of $CaCO_3$ crystals that may have formed over the surface of the calcium hydroxide because of rapid carbonation, which results in a slow hydration rate with time. Additionally, in G1 this BW is slightly less than that of its 7-day content which is most likely because of polymerized C–S–H (or HD-CSH) that formed at the expense of chemically bound water released. Simultaneously, calcium carbonate deposits in the pores of the cement matrix because of early-onset increased reaction kinetics. As a result, diffusion of CO_2 is constrained to enter the uncarbonated zone, which lowers BW in carbonated cement paste with the addition of a high concentration of GO.

However, it should be noted that combined water can be present in two ways in GO-blended cement paste: first, chemically bonded water with hydration products such as C–S–H, CH, ettringite, and more, second, the amount of water adsorbed within the interlayer of graphene oxide [31]. Due to the presence of hydroxy functional groups on the graphene nanosheets, it is typically hydrophilic in nature and the amount of adsorbed inter-layer cannot be removed completely after drying [32]. According to a report, GO aggregates retain a significant quantity of water and lose weight by around 15% when heated to 150 °C [33]. Although we only used a very little amount of GO in our study, the water-bonded with GO agglomerates should still be taken into consideration, especially when using a high amount of GO (1%). Using a mini slump-flow test 12% reduction in slump diameter was observed, which caused stiffness in GO-blended cement paste as compared to plain cement and it confirms that the GO adsorbed some fraction of water. Consequently, measuring combined water by TGA may provide an overestimation of hydration.

Based on equation (2), DOH was calculated for GO-added cement paste in carbonated and uncarbonated conditions at the age of 28 days. Fig. 3 (a) illustrated that in uncarbonated conditions DOH increased about 5–7% with the addition of graphene oxide due to the nucleation effect of GO sheets, which promote the hydration of cement and thus generate more hydration products with time. However, in carbonated condition, G05 showed an increase of ~8.3%, which is attributed to the continuous hydration and formation of C–S–H, CH along with calcium carbonate through the adsorption of CO_2 by graphene oxide sheets, while in G1, the DOH dropped down by 4.3% compared to G05, but still marginally higher than plain cement (Fig. 3(b)). This demonstrated that the early refinement of the cement microstructure due to the addition of high doses of graphene oxide hindered CO_2 diffusion in the cement system. The carbonates that formed on the surfaces of the hydration products and the anhydrous cement as a result of the accelerated CO_2 curing may have further inhibited the dissolution of the cement phases and slowed down the formation of new hydration products.

3.3. Compressive strength

The compressive strength for mixes at 7 and 28 d after removing the samples from the water and CO_2 curing chamber were tested, and the results are illustrated in Fig. 4. At 7-day, with G05 and G1, compressive strengths were found to be 83% and 95% higher compared to plain cement in uncarbonated specimens. This is attributed to the nucleation effect of oxygenated graphene oxide at an early age of hydration, which lowers the porosity by filling the voids associated with the hydration products and considerably increases compressive strength. With the progress of hydration time, compressive strength increment in plain cement from 7 to 28 days is observed superior, which may be attributed to the presence of sufficient initial water-occupied space for hydration product formation. While in GO-blended mixes from 7 to 28 days, this rate of increase is slightly lower than control. This observation revealed that well-dispersed graphene oxide accelerated the hydration mechanism at an early age of hydration and due to space-filling and better packing of the cement matrix, the rate of increasing strength slows down at a later age. Even after, an increase of 15–16% in compressive strength for GO-blended matrix was observed compared to the reference sample without GO at 28 days (Fig. 4).

The availability of pores, which serve as a channel for CO_2 ingression into the cement matrix and contribute to calcium carbonate

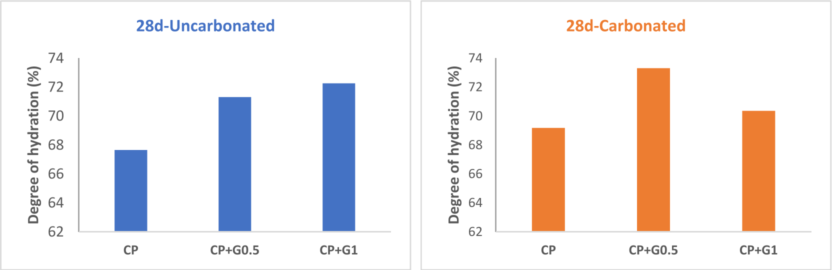

Fig. 3. Degree of hydration (DOH) of graphene oxide incorporated cement under the uncarbonated and carbonated conditions.

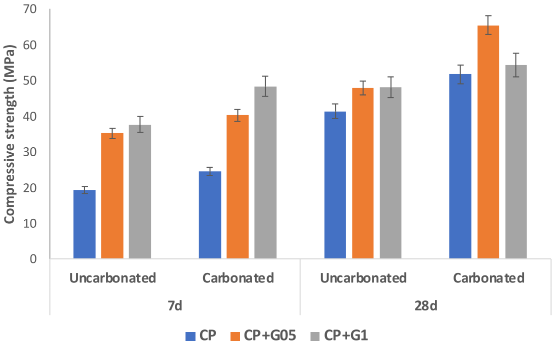

Fig. 4. Compressive strength of uncarbonated and carbonated samples at 7 and 28 days.

precipitation, primarily controls the diffusivity of CO_2 in the cement matrix. The growth of stiffness and strength is significantly impacted by accelerated carbon curing based on the time of exposure. For the carbonated specimens, on the 7th day, it can be clearly observed from Fig. 3, that by adding graphene oxide G05 and G1, compressive strengths increased to 40% and 97%, respectively, as compared to plain cement. This is attributed to the formation of calcium carbonate microcrystals, which results in the filling of micropores and densification of cement matrix. The space between the layered structure and oxygenated edge allowed the interlocking of calcium ions (Ca^{2+}) with graphene sheets and form calcium carbonate on reacting with the dissolved carbonates (CO_3^{2-}). Pore-filling is responsible for this increase in strength, and possibly the combination of $CaCO_3$ with C–S–H may have resulted in the formation of a stronger calcium-silicate-hydrocarbonate binding phase, this finding is also in line with the literature [34]. Fig. 5 presented the denser microstructure of GO-blended paste after carbonation, where calcium carbonate crystals appear to be embedded within the hydration products. EDX graph displayed the collective elemental composition of the highlighted area, and it also confirms the presence of carbonates with the C–S–H, CH, and other hydration products.

Fig. 6 is showing the relative change in the strength of G05 and G1 compared to their counterpart uncarbonated specimens. At 7 days, an increase of 14% and 28% were observed for G05 and G1, respectively, which were attributed to the formation of calcium carbonates. In G05 this relative change is less than G1 because GO was dispersed effectively at a small amount, hence it improved the strength as well as microstructure significantly under water curing and densification of microstructure leads to improve mechanical properties. After prolonged carbonation for 28 days, the compressive strength increased with the amount of graphene oxide up to 0.05%, probably due to residual HD-CSH. Literature suggested that during cement hydration, there is a possibility of forming two types of C–S–H based on their density i.e LD and HD C–S–H. LD-CSH (or outer C–S–H) is highly prone to carbonate quickly and resulting in disintegration into $CaCO_3$. The initial layer of $CaCO_3$ acts as a barrier and stops the inward ingress of CO_2, which prevent interior C–S–H (or inner C–S–H) from carbonating [35]. Based on this, it can be assumed that after extended exposure to the CO_2 environment, the development of the $CaCO_3$ layer inhibited further carbonation of C–S–H and a considerable amount of HD-CSH leftover, which helped in improving the mechanical strengths of cement-based composites. Although with 0.1% of GO, a reduction in compressive strength was observed compared to 0.05% GO addition, however, it is still higher than the control sample. This can be explained by forming a denser microstructure of the G1 mix at an early age. Thus, with the increased time of carbonation, there was no longer pore

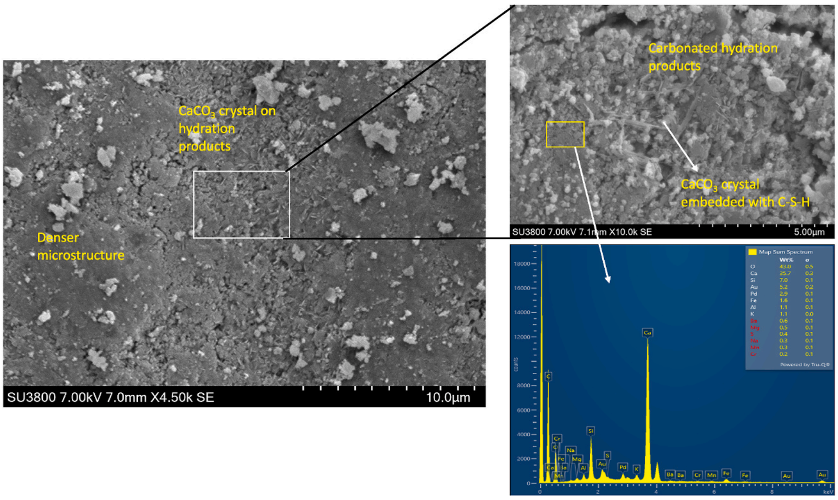

Fig. 5. SEM micrograph and elemental composition of carbonated graphene oxide blended paste.

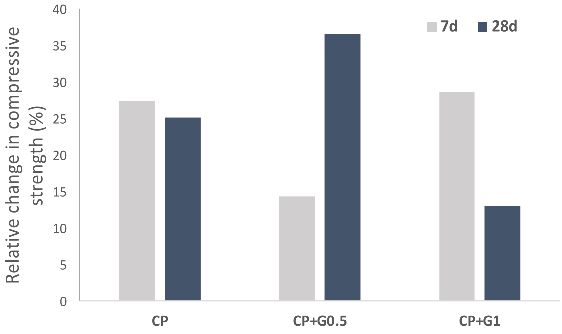

Fig. 6. Relative change in compressive strength of CO_2 cured samples w.r.t uncarbonated samples.

space remained for new precipitates to occupy, and then the carbonates started to accumulate on the surfaces of hydration products. Eventually, this accumulation caused brittleness to the specimens, and due to expansion microcracks developed in the carbonated zones [36]. This is also in agreement with BW and DOH results, on carbonation, the amount of hydration products decreased in G1 compared to G05.

3.4. CO_2 sequestration by graphene oxide modified cementitious system

3.4.1. Zeta potential and interaction mechanism of GO and $Ca(OH)_2$ under carbonation condition

Zeta potential is a helpful surface characteristic for comprehending how particle surfaces interact with the surrounding medium. Dispersion of graphene oxide in an aqueous solution yielded apparently stable solutions. However, the zeta potential was also measured to quantify the suspension stability, which is considered acceptable when the zeta potential absolute value is higher than 30 mV [37].

GO solution presented a negative Zeta potential absolute value of 42 mV (shown in Fig. 7), indicating a stable and homogeneous suspension, displayed in Fig. 8(B). The effect of a high pH environment on the stability of GO dispersion was investigated using a saturated solution of $Ca(OH)_2$ (observed zeta potential of 0.4 mV) depicted in Fig. 8(A) to imitate the highly alkaline cementitious pore solution separately. Thereafter, to the stable water dispersed solution of GO, a saturated solution of $Ca(OH)_2$ solution was added (Fig. 8 (C)), and the zeta potential value was recorded. From this study, it was observed that the zeta potential of the mixture shifted from −42 mV to −10mV. It might happen due to the interaction of calcium cations (Ca^{2+}) to the negative surface of GO (OH^-, COO^-), which caused an increase in the surface charge of GO, and subsequently leads to a positive surface. Similarly, when cement encounters water, dissolution of ions starts, and Ca^{2+} ions are soon adsorbed on the surface of graphene oxide, increasing the zeta potential value. After a while due to the high surface area and strong affinity of GO to positive ions, its surface eventually gets saturated with interlocked Ca^{2+} ions. This process increases the mobility of ions in cement pore solution, which greatly increases the interaction of intercalated Ca^{2+} with the surface of cement particles and encourages nucleation and growth of hydration product on the cement surface, supported by the degree of hydration results in section 3.2.

When the solution of individual GO, CH, and combined GO + CH was subjected to carbonation for 24 h, white precipitation of $CaCO_3$ was observed in both the solution of individual CH (Fig. (8(D)) and combined GO + CH (Fig. 8(f)). In GO solution, the settling of graphene oxide is probably due to keeping undisturbed for a long time (Fig. 8(E)). As mentioned earlier, a superplasticizer was not used to prepare these solutions, therefore after 24 h, GO began to settle at the bottom. A similar type of behavior was observed after 24 h without carbonation.

Likewise, when carbon dioxide diffuses in the cement matrix containing graphene oxides, it reacts with interlocked calcium ions and forms carbonate ions (CO_3^{2-}). In this study, the increased positive charge of GO sheets may lead to the attraction of negatively

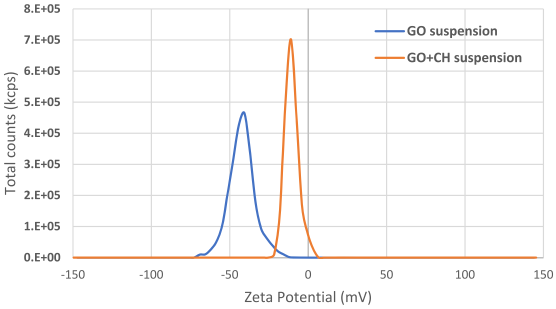

Fig. 7. Zeta potential of GO and GO + CH solutions.

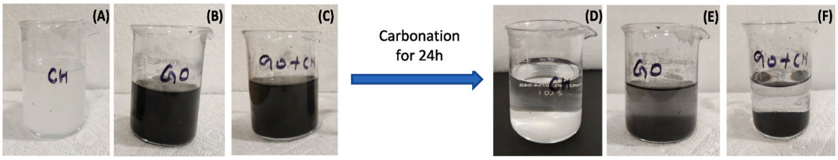

Fig. 8. Images of solutions for CH, GO, and combined GO + CH kept in uncarbonated (A, B,C) and Carbonated conditions (D, E, F).

charged carbonate ions and result in more $CaCO_3$ precipitation compared to plain cement. This proposed mechanism presented in Fig. 9, helped in the permanent mineralization of atmospheric carbon dioxide by employing GO in the cementitious system. This occurrence is verified in the later sections 3.4.2 and 3.4.3, based on the estimation of calcium carbonate and CH content upon carbonation.

3.4.2. CH consumption

Fig. 10 (a and b) illustrated the 7th day TG curves of the GO-blended cement pastes cured under water and CO_2 environment. The weight loss in paste samples can be observed mainly in three regions. First, the weight loss in the temperature range between 20 °C and 105 °C is corresponding to the loss of physically absorbed water from the accessible pore network of cement composites. Second, the weight loss in the region between 400 °C and 500 °C is attributed to the dihydroxylation of calcium hydroxide. Under carbonation, which is much less intense as a result of the carbonation of calcium hydroxide and transformation to calcium carbonate (Fig. 10(b)). Third, the region between 650 °C and 900 °C is mainly for the decomposition of different polymorphs of calcium carbonates, which demonstrated a significant peak intensity due to the carbonation of hydration products. In contrast to normal cement paste, the change in peak intensities in GO-blended paste varied dramatically due to different hydration and carbonation reaction mechanism.

The amount of $CaCO_3$ (g/100 g) and CH(g/100 g) was obtained directly from TGA curves by using Eqs (3) and (4). Fig. 11 (a and b) show the amount of CH in uncarbonated and carbonated pastes samples. From Fig. 11(a), it was observed that the amount of CH in G05 is 5.9% lower than the plain cement under uncarbonated conditions, which may be explained by the interlocking of calcium ions within oxygenated layers of graphene oxide, as explained earlier in section 3.4.1. This reaction will reduce the concentration of Ca^{2+} in pore solution and precipitates less amount of calcium hydroxide at 7 days. While with the continuous hydration when the sites on GO-sheets are fully occupied, then the available calcium ions react with hydroxides ions in pore solution and continue to form CH, therefore at 28 days CH content increased. However, in carbonated conditions, the reduction in CH content is observed higher especially in the G05 mix at 7 days of carbonation. This could be attributed to the rapid CH reactivity with carbon dioxide at the early age of accelerated carbonation. Graphene oxides are usually hydrophilic and carbonaceous materials, which are naturally good at CO_2 adsorption due to the interconnected layers with significant oxygen content [38]. As the carbonation continues till 28 days, it can be observed that this amount is increased compared to the 7 days of carbonation. This might be a result of early exposure to high CO_2 environments and the increased hydration of cement in the presence of GO. When fresh specimens were carbonated, it caused a rapid reaction of CH with carbon dioxide, covering the surface of CH and anhydrous cement with calcium carbonate crystals [39]. The fact that the quantity of CH in the G1-blended cement mix has hardly changed might be attributed to the carbonates that have accumulated over hydration products, which have further inhibited the interaction of CO_2 with calcium hydroxide and prevented CH from carbonating even after prolonged carbonation. From Fig. 11(b), it is interesting to be noted that on carbonation CH content is still higher than plain cement, which showed that the addition of GO might prevent the drastic reduction of pH or alkalinity of the cement matrix while improving mechanical performance and carbonate mineralization.

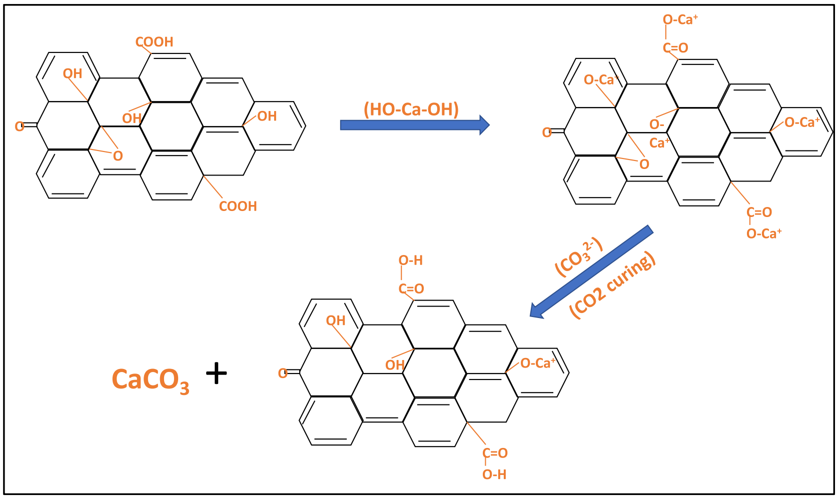

Fig. 9. Schematic representation of reaction mechanism of GO in alkaline medium.

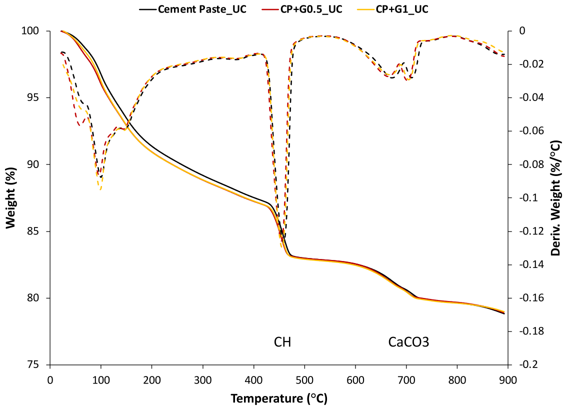

Fig. 10a. TGA curves of uncarbonated cement paste with GO at 7 days.

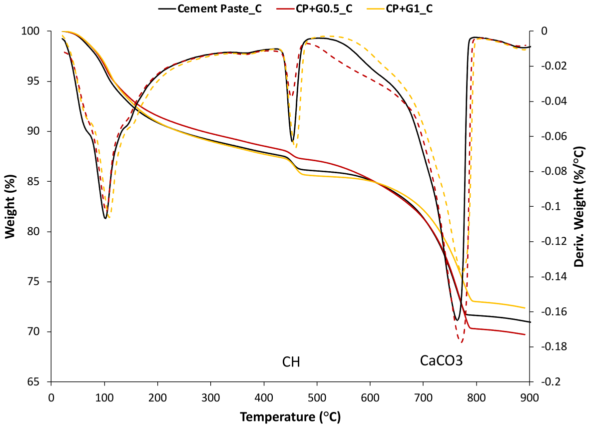

Fig. 10b. TGA curves of carbonated cement paste with GO at 7 days.

Adding graphene oxide, a large number of Ca^{2+} were chemically linked, either face-to-face or edge-to-edge of GO nanosheets. Also, reported in the study [40] that about 25% of weight loss was observed in the temperature range from 300 to 500 °C, and is attributed to the elimination of oxygen-containing functional groups. Therefore, it is reasonable to assume that some of the weight loss experienced by GO-blended cement paste across the temperature range of 400–500 °C was caused by the removal of cross-linked Ca^{2+} ion bonded with oxygen-containing functional groups (OH and COOH). To confirm the effect, XRD graphs of 7 days were obtained for uncarbonated and carbonated pastes incorporating GO, presented in Fig. 12. XRD graph showed that the corresponding peak intensity of CH at 18.2 (2θ) is relatively higher in G05 than control in uncarbonated cement paste, whereas on carbonation this peak significantly decreased and the major peak of calcite at 29.5 (2θ) increased due to converting CH into $CaCO_3$. Further, as GO concentration increased to 0.1%, rapid deposition of a crystalline layer of calcium carbonates in CH surrounding reduced the carbonation of calcium hydroxide, resulting in high CH content in G1 mix compared to G05 and plain cement paste.

3.4.3. Carbonate mineralization and CO_2 uptake potential

$CaCO_3$ mineralization in GO-blended cement matrix at 7 and 28 days carbonated samples are presented in Table 4. At 7 days, $CaCO_3$ content was calculated about 32.7% in plain cement paste, which translates to 10.4% of CO_2 uptake. Using a high w/c ratio helps easy mixing and better workability with the additional capillary pores. The availability of free water in the porous network provides sites for the dissolution of carbon dioxide, which is necessary to drive the carbonation reaction [41]. However, with the addition of graphene oxide, $CaCO_3$ content increased to 39.6% corresponds to 13.4% of CO_2 uptake in the cement system, which is about 30% more CO_2 sequestration as compared to plain cement (Fig. 13). The enhanced CO_2 ingress and rapid reactivity with intercalated Ca^{2+} ion with the graphene sheets is linked to this increase in CO_2 sequestration. Due to the continuous precipitation, the cement matrix becomes denser and on increasing GO to 0.1%, CO_2 uptake is reduced (as described in section 3.3).

Moreover, after 28 days of carbonation, this increase in carbonate mineralization and CO_2 uptake continued in plain cement paste due to the availability of space for precipitation of $CaCO_3$. However, the carbonate mineralization potential slows down in GO-added cement paste. The increase in carbonate content from 7 d to 28 d is slower (2.6%) in G05 than plain cement paste (13%) and G1 (20%), which corresponds to 13.6% of CO_2 uptake at 28 days. These results imply that the small addition of GO (0.05%) substantially

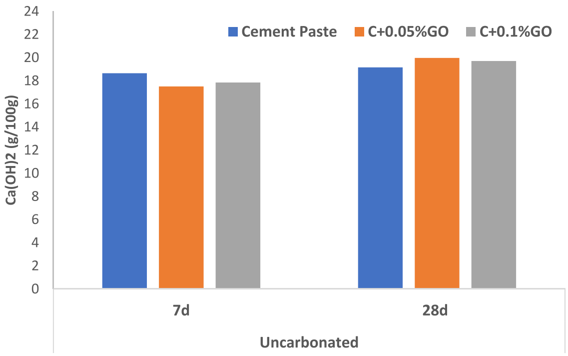

Fig. 11a. TGA results of CH content of uncarbonated GO incorporated paste sample after 7 and 28 days.

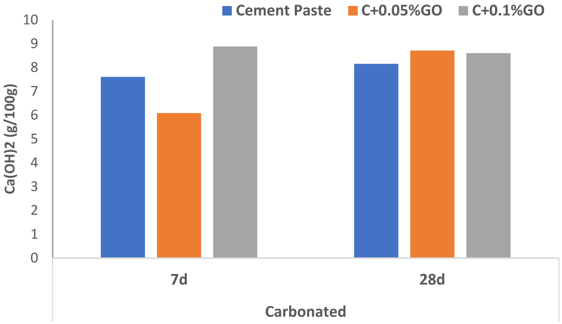

Fig. 11b. TGA results of CH content of carbonated GO incorporated paste sample after 7 and 28 days.

advances the early-age adsorption of CO_2 in cement. Owing to the efficient dispersion at low concentrations, GO accelerated the carbon uptake process and allowed the pore spaces to be refined by calcium carbonate precipitation. Simultaneously, when the pores are filled then the carbonates start depositing over hydration products and anhydrous cement particles. This overgrowth of carbonate crystals on the surfaces limits the chemical reaction between hydration products and CO_2 under continuous CO_2 flow. Further, on increasing the amount of GO, carbonate mineralization and CO_2 uptake potential were reduced, probably due to densification of microstructure and insufficient dispersion of GO sheets. This reduction in mechanical properties has also been observed earlier. Hence, this study suggests that the addition of a small amount of GO in cementitious system can capture and store atmospheric CO_2 effectively with the added benefit of improving mechanical and hydration properties.

3.5. *FTIR spectrum analysis*

FTIR spectra of cement paste with 0.05% and 0.1% of graphene oxide after carbonation till 7 and 28 days are shown in Figs. 14 and 15. The spectra show a remarkably sharp C–O stretching at 872 cm^{-1} and 1418 cm^{-1}, which confirms the carbonation-induced production of a stable form of calcite ($CaCO_3$) in all the mixes [42]. From the spectra, It can be observed that the peak intensity for the calcite is higher in G05 than the plain hydrated cement at 7 days. With the progress of carbonation curing at 28 days, this peak intensity at 1418 cm^{-1} is comparatively higher in GO-blended cement paste. This infers that GO enhanced CO_2 adsorption. However, on increasing the amount of GO, further diffusion of CO_2 was restricted only due to densification of the microstructure. It can be seen from earlier compressive strength results that G1 has improved mechanical properties in uncarbonated conditions.

Additionally, at day 7, the spectra also showed peaks at 965 cm^{-1}, which correspond to the stretching of Si–O bond, suggesting that there had been no apparent change in C–S–H. However, the apparent decrease in the intensity of this band might have been caused due to alternation in C–S–H gel upon carbonation. While at 28 days, with the slight increase in intensity, this band shifted to a higher wave number clearly showing the formation of highly polymerized C–S–H, especially in the G05 mix. The formation of polymerized or denser C–S–H could also be one of the reasons for improving mechanical properties. The broad and small bands at 1664 cm^{-1}, indicated the bending vibrations (H–O–H) and the absorption bands from 3100 to 3500 cm^{-1} correspond to the O–H stretching vibrations in the interlayer water molecules combined with hydration products [43]. The peak at 3648 cm^{-1} corresponds to the presence of CH, which is formed due to accelerated hydration of silicate phases (C_3S and C_2S) in the hydrated cement. When GO is added to the cement paste, the characteristic CH peak intensities at 28 days considerably decrease compared to their intensities in plain cement paste. This discrepancy is probably due to the carbonation of CH in presence of GO. These findings also supported the mechanical and TGA results discussed previously and proved that GO has high reactivity with hydrated cement, leading to improved mechanical performance. In addition, CO_2 sequestration in cement-based materials can also be enhanced significantly with a small addition of GO.

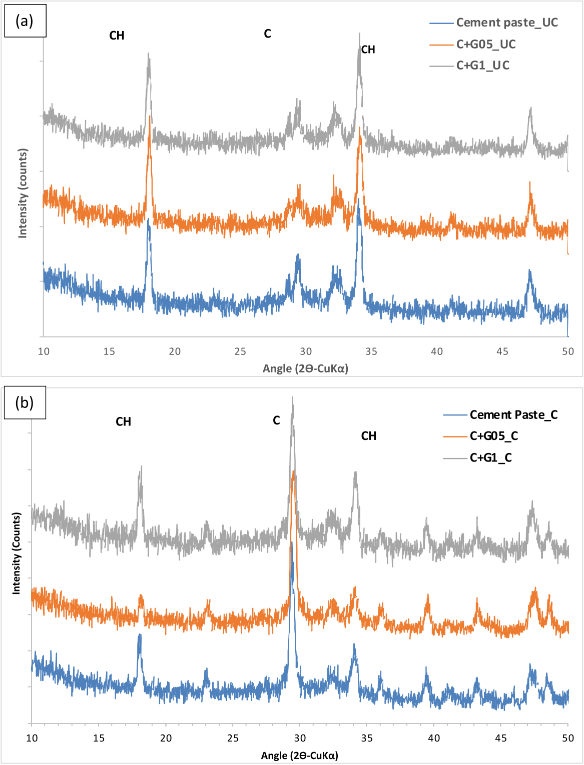

Fig. 12. XRD profile of uncarbonated **(a)** and carbonated **(b)** paste samples at 7 days (CH: calcium hydroxide, C: calcite).

Table 4
$CaCO_3$ content in uncarbonated and carbonated pastes with GO.

	$CaCO_3$ (g/100 g)			
	Uncarbonated		Carbonated	
	7d	**28d**	**7d**	**28d**
Cement Paste	9.1	7.5	32.7	37.1
C+0.05%GO	8.9	8.2	39.6	39.1
C+0.1%GO	8.6	8.2	29.8	35.9

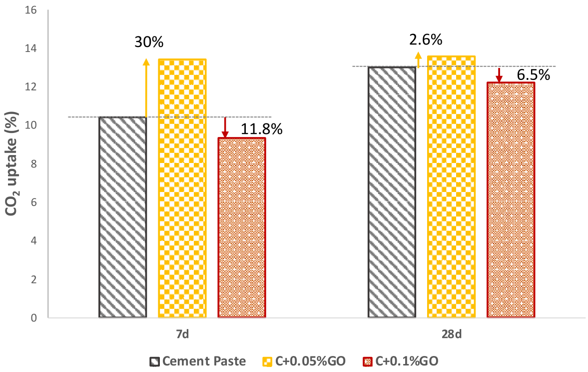

Fig. 13. CO_2 sequestration potential of GO incorporated cement paste samples at 7 and 28 days.

4. Conclusions

The effect of graphene oxide on CO_2 sequestration, hydration kinetics, and strength development was investigated and the following conclusions were observed:

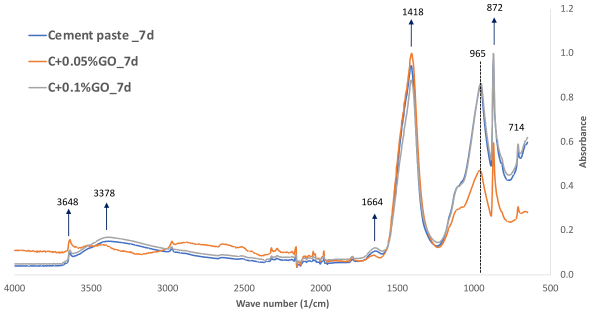

Fig. 14. FTIR spectrum of graphene oxide incorporated cement after carbonation at 7 day.

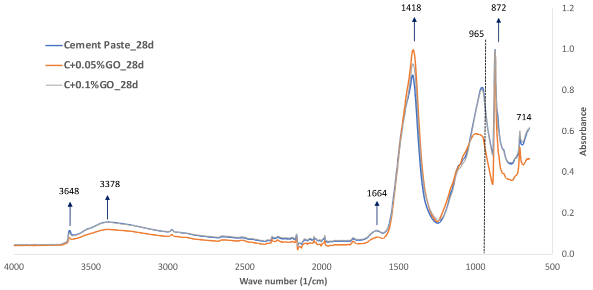

Fig. 15. FTIR spectrum of graphene oxide incorporated cement after carbonation at 28 day.

- The additional benefit of using graphene oxide in a cementitious system is that it can be used for CO_2 sequestration; it has the potential to increase CO_2 uptake by 30% with a very small amount of graphene oxide (0.05%), while maintaining its structural integrity in comparison to plain cement-based materials.
- In an alkaline environment, an increase in zeta potential facilitated the reactivity of carbonates on the surface of GO and enhanced CO_2 sequestration in the microstructure of GO-cement.
- The presence of oxygen-containing functional groups on the surface of graphene oxide nanosheets facilitated the interaction of dissolved ions in pore solution with GO and accelerated hydration kinetics, which led to the precipitation of additional hydration products.
- Chemically bound water and degree of hydration are improved by 8.3% at 28 days on G05 addition, while at higher amounts of GO, DOH was controlled due to the refinement of microstructure.
- Compressive strength in G05 and G1 significantly increased at 7 days under both curing conditions, whereas at 28 days, on prolonged carbonation, the compressive strength of the G1 blended mix decreased due to the deposition of carbonates crystals on hydration products, which further hindered the hydration mechanism.
- The simultaneous occurrence of carbonation and hydration process caused the $CaCO_3$ and calcium hydroxide concentration to be higher in the G05-cement matrix in comparison to plain cement, which demonstrated the potential of graphene oxide for storing CO_2 and maintaining the pH of the cementitious system at the same time.

CRediT authorship contribution statement

Geetika Mishra: Conceptualization, Methodology, Formal analysis, Investigation, Writing – original draft, Data curation. **Ashraf Warda:** Resources, Supervision, Validation, Writing – review & editing. **Surendra P. Shah:** Conceptualization, Resources, Supervision, Project administration, Funding acquisition, Writing – review & editing.

Declaration of competing interest

The authors declare that they have no known competing financial interests or personal relationships that could have appeared to influence the work reported in this paper.

Data availability

Data will be made available on request.

Acknowledgment

The authors Geetika Mishra is thankful to the Center for Advanced Construction Materials (CACM), the University of Texas at Arlington for project funding and Warda Ashraf acknowledges the support from the US National Science Foundation (NSF # ECI - 2028462). All opinions, findings, and conclusions or recommendations expressed in this research paper are those of the authors and do not necessarily reflect the views of the funding agencies.

References

[1] S. Lv, Y. Ma, C. Qiu, T. Sun, J. Liu, Q. Zhou, Effect of graphene oxide nanosheets of microstructure and mechanical properties of cement composites, Construct. Build. Mater. 49 (2013) 121–127.
[2] H.B. Yang, H.Z. Cui, W. Tang, Z.J. Li, N.X. Han, F. Xing, A critical review on research progress of graphene/cement based, Compos. Part A. 102 (2017) 273–296.
[3] T.M. Sheikh, M.P. Anwar, K. Muthoosamy, J. Jaganathan, A. Chan, A.A. Mohamed, The mechanics of carbon-based nanomaterials as cement reinforcement — a critical review, Construct. Build. Mater. 303 (2021), 124441.
[4] H. Yang, H. Cui, W. Tang, Z. Li, N. Han, F. Xing, A critical review on research progress of graphene/cement-based composites, Compos. Part Appl. Sci. Manuf. 102 (2017) 273–296.
[5] M. Krystek, D. Pakulski, V. Patroniak, M. Górski, L. Szojda, A. Ciesielski, P. Samorì, High-performance graphene-based cementitious composites, Adv. Sci. 6 (2019), 1801195.
[6] Qin Wang, Guo-dong Qi, Yue Wang, Hai-yu Zheng, Si-han Shan, Chun-xiang Lu, Research progress on the effect of graphene oxide on the properties of cement-based composites, N. Carbon Mater. 36 (4) (2021) 729–750.
[7] E. Worrell, L. Price, N. Martin, C. Hendriks, L.O. Meida, Carbon dioxide emissions from the global cement industry, Annu. Rev. Energy Environ. 26 (1) (2001) 303e329.
[8] X. Shi, Y. Yao, L. Wang, C. Zhang, I. Ahmad, A modified numerical model for predicting carbonation depth of concrete with stress damage, Construct. Build. Mater. 304 (2021), 124389.
[9] V.G. Papadakis, Effect of supplementary cementing materials on concrete resistance against carbonation and chloride ingress, Cement Concr. Res. 30 (2) (2000) 291–299.
[10] D. Ramachandran, S. Uthaman, V. Vishwakarma, Studies of carbonation process in nanoparticles modified fly ash concrete, Construct. Build. Mater. 252 (2020), 119127.
[11] A. Dindi, D.V. Quang, L.F. Vega, E. Nashef, M.R.M. Abu-Zahra, Applications of fly ash for CO2 capture, utilization, and storage, J. CO2 Util. 29 (2019) 82–102.
[12] C. Moro, V. Francioso, M. Velay-Lizancos, Impact of nano-TiO2 addition on the reduction of net CO2 emissions of cement pastes after CO2 curing, Cem. Concr. Compos. 123 (2021), 104160.
[13] S. Von Greve-Dierfeld, B. Lothenbach, A. Vollpracht, et al., Understanding the carbonation of concrete with supplementary cementitious materials: a critical review by RILEM TC 281 CCC, Mater. Struct. 53 (2020) 136.
[14] D. Zhang, Z. Ghouleh, Y. Shao, Review on carbonation curing of cement-based materials, J. CO2 Util. 21 (2017) 119, 13.
[15] A.N. Junior, , Romildo Dias Toledo Filho, Eduardo de Moraes Rego Fairbairn, Jo Dweck, The effects of the early carbonation curing on the mechanical and porosity properties of high initial strength Portland cement pastes, Construct. Build. Mater. 77 (2015) 448–454.
[16] Y. Shao, M.S. Mirza, X. Wu, CO2 sequestration using calcium–silicate concrete, J. Civ. Eng. 33 (2006) 776.
[17] Y. Shao, X. Zhou, S. Monkman, A New CO2 Sequestration Process via Concrete Products Production, Department of Civil Engineering, McGill University, Montreal, 2006.
[18] J. Wang, H. Xu, D. Xu, P. Du, Z. Zhou, L. Yuan, X. Cheng, Accelerated carbonation of hardened cement pastes: influence of porosity Construct, Build. Mater. 225 (2019) 159–169.
[19] A. Morandeau, M. Thiéry, P. Dangla, Investigation of the carbonation mechanism of CH and C-S-H in terms of kinetics, microstructure changes and moisture properties, Cement Concr. Res. 56 (2014) 153–170.
[20] K. Adamczyk, M. Prémont-Schwarz, D. Pines, E. Pines, E.T.J. Nibbering, Real-time observation of carbonic acid formation in aqueous solution, Science 326 (2009) 1690–1694.
[21] H. Qin, W. Wei, Y. Hang Hu, Synergistic effect of graphene-oxide-doping and microwave curing on mechanical strength of cement, J. Phys. Chem. Solid. 103 (2017) 67–72.
[22] Q. Wang, J. Wang, C. Lu, et al., Influence of graphene oxide additions on the microstructure and mechanical strength of cemen, N. Carbon Mater. 30 (4) (2015) 349–356.
[23] M. Elsalamawy, A.R. Mohamed, E.M. Kamal, The role of relative humidity and cement type on carbonation resistance of concrete, Alex. Eng. J. 58 (4) (2019) 1257–1264.
[24] A. Leemann, F. Moro, Carbonation of concrete: the role of CO 2 concentration, relative humidity and CO 2 buffer capacity Mater, Structure 50 (1) (2017) 30.
[25] J. John, K. Hirai, H. Mihashi, Influence of environmental moisture and temperature on carbonation of mortar Concr, Respir. Technol. 1 (1) (1990) 85–94.
[26] G. Mishra, A.C. Emmanuel, S. Bishnoi, Influence of temperature on hydration and microstructure properties of limestone-calcined clay blended cement, Mater. Struct. 52 (2019) 91.
[27] J.I. Bhatty, K.J. Reid, Use of thermal analysis in the hydration studies of a type 1 portland cement produced from mineral tailings, Thermochim. Acta 91 (1985) 95–105.
[28] R.H. Bogue, The Chemistry of Portland Cement, second ed., Reinhold Publishing Corporation, Washington, DC, USA, 1955.
[29] H. M, X. Jia, K.H. Mo, T.C. Ling, Effect of water-to-cement ratio induced hydration on the accelerated carbonation of cement pastes, Environ. Pollut. 280 (2021), 116914.
[30] W. Li, X. Li, S.J. Chen, et al., Effects of graphene oxide on early-age hydration and electrical resistivity of Portland cement paste, Construct. Build. Mater. 136 (2017) 506–514.
[31] N.V. Medhekar, A. Ramasubramaniam, R.S. Ruoff, V.B. Shenoy, Hydrogen bond networks in graphene oxide composite paper: structure and mechanical properties, ACS Nano 4 (4) (2010) 2300–2306.
[32] D.A. Dikin, S. Stankovich, E.J. Zimney, R.D. Piner, G.H. Dommett, G. Evmeneno, etal, Preparation and characterization of graphene oxide paper, Nature 448 (7152) (2007) 457–460.
[33] J. Gao, C. Liu, L. Miao, X. Wang, Y. Chen, Free-standing reduced graphene oxide paper with high electrical conductivity, J. Electron. Mater. (2015) 1–6.
[34] S. Gupta, Carbon sequestration in cementitious matrix containing pyrogenic carbon from waste biomass: a comparison of external and internal carbonation approach, J. Build. Eng. 43 (2021), 102910.
[35] G. Groves, D. Rodway, I. Richardson, The carbonation of hardened cement pastes, Adv. Cement Res. 3 (11) (1990) 117–125.
[36] M. Fernández Bertos, S.J. Simons, C.D. Hills, P.J. Carey, A review of accelerated carbonation technology in the treatment of cement-based materials and sequestration of CO2, J. Hazard Mater. 112 (3) (2004) 193–205.
[37] M.J. Vold, Zeta potential in colloid science. Principles and applications, J. Colloid Interface Sci. 88 (1982) 608.
[38] D. Kim, D.W. Kim, H. K Lim, J. Jeon, H. Kim, H.T. Jung, H. Lee, Intercalation of gas molecules in graphene oxide interlayer: the role of water, J. Phys. Chem. 118 (20) (2014) 11142–11148.
[39] B. Savija, M. Lukovic, Carbonation of cement paste: understanding, challenges, and opportunities, Construct. Build. Mater. 117 (2016) 285–301.
[40] Xiangyu Li, Zeyu Lu, Samuel Chuah, Wengui Li, Yanming Liu, Wen Hui Duan, Zongjin Li, Effects of graphene oxide aggregates on hydration degree, sorptivity, and tensile splitting strength of cement paste, Compos. Part A Appl. Sci. 100 (2017) 1–8.

[41] B. Šavija, M. Luković, Carbonation of cement paste: understanding, challenges, and opportunities Construct, Build. Mater. 117 (2016) 285–301.

[42] W. Li, F. Qu, W. Dong, G. Mishra, S.P. Shah, A comprehensive review on self-sensing graphene/cementitious composites: a pathway toward next-generation smart concrete, Construct. Build. Mater. 331 (2022), 127284.

[43] S. Yaseen, G. Yiseen, Z. Li, Elucidation of calcite structure of calcium carbonate formation based on hydrated cement mixed with graphene oxide and reduced graphene oxide, ACS Omega 4 (2019) 10160–10170.